Nanotechnology **19** (2008) 075610 (6pp) doi:10.1088/0957-4484/19/7/075610

Magnetic sensitivity enhanced novel fluorescent magnetic silica nanoparticles for biomedical applications

Jaemoon Yang[1], Jaewon Lee[1], Jinyoung Kang[1,2], Chan-Hwa Chung[3], Kwangyeol Lee[4], Jin-Suck Suh[2,5], Ho-Geun Yoon[6], Yong-Min Huh[2,5,7] and Seungjoo Haam[1,2,7]

[1] Department of Chemical Engineering, Yonsei University, Seoul 120-749, Korea
[2] Graduate Program for Nanomedical Science, Yonsei University, Seoul 120-749, Korea
[3] Department of Chemical Engineering, Sungkyunkwan University, Suwon 440-746, Korea
[4] Department of Chemistry, Korea University, Seoul 136-701, Korea
[5] Department of Radiology, College of Medicine, Yonsei University, Seoul 120-752, Korea
[6] Department of Biochemistry and Molecular Biology, Center for Chronic Metabolic Disease Research, College of Medicine, Yonsei University, Seoul 120-752, Korea

E-mail: ymhuh@yumc.yonsei.ac.kr and haam@yonsei.ac.kr

Received 1 November 2007, in final form 20 December 2007
Published 31 January 2008
Online at stacks.iop.org/Nano/19/075610

Abstract
We synthesized novel fluorescent magnetic silica nanoparticles (FMSNPs) containing large magnetic components for biomedical application. By employing assemblies of magnetic nanoparticles as kernels against FMSNPs, both the saturation of magnetization and the magnetic resonance (MR) signal intensity were significantly enhanced. Furthermore, the cellular binding of FMSNPs was improved by introducing a positive charge on the surface of the FMSNPs, and fluorescent dyes on the surface of FMSNPs enable optical imaging of sub-cellular regions.

(Some figures in this article are in colour only in the electronic version)

1. Introduction

The magnetic properties of magnetite nanoparticles (MNPs) have been widely studied for various biomedical applications, such as targeted drug delivery [1], cell labeling [2], cell separation [3], immunoassay [4], magnetic resonance imaging (MRI) [5–7], and magnetic hyperthermia [8]. Of all magnetic substances, magnetite (Fe_3O_4) is the most applicable material due to its biocompatibility in the human body and high magnetic sensitivity under magnetic field. In general, MNPs can be synthesized by co-precipitation [9, 10] or thermal decomposition methods [1, 11]. In particular, the thermal decomposition method is the preferred method for the synthesis of monodisperse MNPs and their high magnetic sensitivity [5, 6]. Due to their relatively low colloidal stability in medium pH, however, surface modifications of MNPs should be carried out to increase the physico-chemical stability and biofunctionality [9, 10]. In order to apply MNPs as functional delivery carriers and separation agents, therefore, magnetic nanoparticles coated with a silica shell are desirable because the silica can be easily synthesized and it can functionalize the surface with amine, carboxyl, aldehyde and thiol groups [12]. Furthermore, fluorescent dyes can be introduced to magnetic silica nanoparticles for optical and magnetic resonance (MR) imaging of target cells [12, 13]. The MR imaging technique can analyze interrogated subjects with high spatial resolution, and it is a non-invasive method. Moreover, optical imaging using fluorescent dyes can give a microscale image due to the remarkable sensitivity. In general, the Stöber method using tetraethyl orthosilicate (TEOS) has been adopted widely for the preparation of silica-coated magnetic nanoparticles because of its advantages compared with the other methods, i.e. it needs relatively mild reaction conditions, is of low cost and is surfactant free [9, 10]. However, the preparation

[7] Authors to whom any correspondence should be addressed.

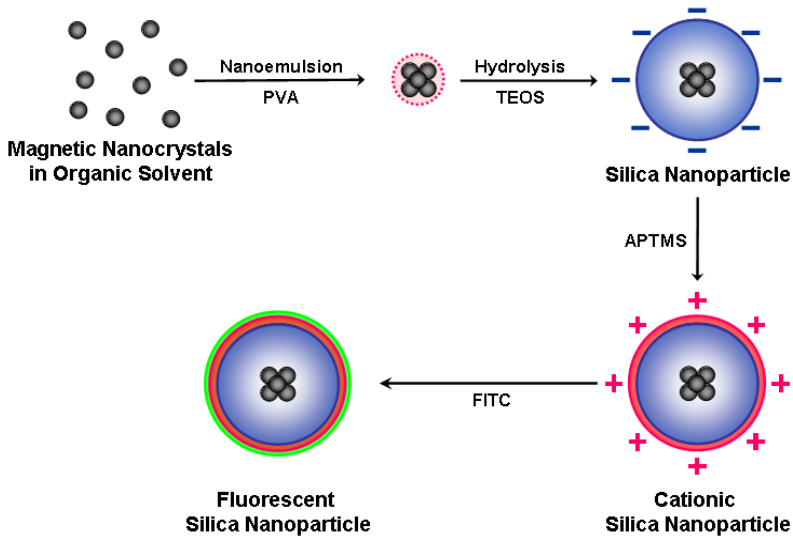

Figure 1. Conceptual scheme for the preparation of fluorescent magnetic silica nanoparticles (FMSNPs).

of magnetic silica nanoparticles containing large amounts of magnetic substances was considerably difficult. Previous studies showed irregular structures and morphologies of magnetic silica nanocomposites and it was hard to control the magnetic material contents. Irregular-sized magnetic silica nanoparticles were produced due to the absence of a seed pretreatment.

In this study, thus, we now report the synthesis and characterization of fluorescent magnetic silica nanoparticles (FMSNPs) for multimodal imaging and separation of target cells using ionic interaction. The monodisperse magnetic nanoparticles were synthesized by thermal decomposition methods and the magnetic assemblies were prepared with a stabilizer (polyvinylalcohol) using a nanoemulsion method [1]. Magnetic assemblies as kernels were covered with a silica outer layer by the Stöber method. Hydrolysis and condensation of TEOS induced the silica shell that increased the colloidal stability and biofunctionality for biomedical applications [4, 12]. To increase the cell binding efficiency, a cationic surface modification process was carried out. After conjugation of a fluorescent dye on the surface of magnetic silica nanoparticles, a cell affinity test was carried out, and MR signal-enhancing effects were investigated to assess the potential of FMSNPs for biomedical applications.

2. Materials and methods

2.1. Materials

Iron (III) acetylacetonate, 1,2-hexadecanediol, dodecanoic acid, dodecylamine, benzyl ether, 3-aminopropyl trimethoxy silane (APTMS) and polyvinylalcohol (M_W: 15 000–20 000 Da) were purchased from the Sigma-Aldrich Chemical Co. (USA). Fluorescein isothiocyanate (FITC) was obtained from Fluka. All other chemicals and reagents were of analytical grade.

2.2. Synthesis of magnetic kernels (MKs)

The synthesis of monodisperse magnetic nanoparticles (MNPs) was started from a mixture of iron (III) acetylacetonate (4 mmol), 1,2-hexadecanediol (20 mmol), dodecanoic acid (12 mmol), dodecylamine (12 mmol), and benzyl ether (50 ml). The mixture was preheated to 120 °C for 30 min under nitrogen atmosphere and refluxed at 300 °C for 1 h. After the reactants were cooled to room temperature, the products were purified with pure ethanol. 12 nm of MNPs were synthesized after the seed-mediated growth. To prepare the magnetic kernels (MKs), 5 mg of MNPs were dissolved in 4 ml of chloroform. This organic phase was added into 10 ml of aqueous phase containing 200 mg of polyvinylalcohol (PVA) [1]. After mutual saturation of the organic and continuous phase, the mixture was emulsified for 10 min with an ultrasonicator (ULH700S, Ulssohitech, Korea) at 200 W. After evaporation of the organic solvent, the products were purified by filtration and centrifugation at 21k rpm.

2.3. Synthesis of fluorescent magnetic silica nanoparticles (FMSNPs)

The magnetic silica nanoparticles (MSNPs) containing MKs were synthesized by the modified Stöber method [9, 14]. For synthesizing MSNPs, MKs act as seeds in a mixture of alcohol and water at ambient temperature. 1 ml of MKs (5 mg ml^{-1}) was diluted with 4 ml ethyl alcohol and 0.1 ml ammonia solution (28% in water). TEOS (60 μl) was slowly added to this suspension, and after stirring for 12 h, a silica outer shell formed on the surface of MKs through hydrolysis and condensation of TEOS. The synthetic procedure of MSNPs is illustrated in figure 1.

In order to conjugate a fluorescent dye with the MSNPs, amine terminated MSNPs (AMSNPs) were synthesized using 3-aminopropyl trimethoxy silane (APTMS) [15, 16]. 10 mg of MSNPs in suspension were added to 0.1 ml of 3-aminopropyl trimethoxysilane in deionized water. The mixture was reacted

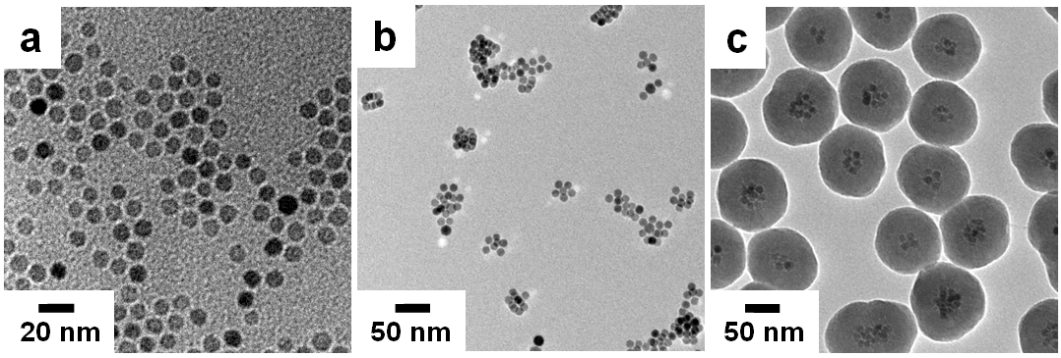

Figure 2. TEM images of (a) magnetic nanoparticles (MNPs), (b) magnetic kernels (MKs) and (c) magnetic silica nanoparticles (MSNPs).

with vigorous stirring at 90 °C for 24 h. The products were washed several times with centrifugation. Then, for fabrication of fluorescent MSNPs (FMSNPs), 0.5 ml of FITC solution (2 mg ml^{-1}) was mixed with AMSNPs (10 mg) for 2 h in a dark room. The unwanted materials were removed using centrifugation three times.

2.4. Characterizations

The morphology and size distribution were evaluated with a transmission electron microscope (TEM; JEM-2100, JEOL Ltd). The size distribution and surface charge of MNPs, MKs, MSNPs and FMSNPs were analyzed by laser scattering (ELS-Z, Otsuka electronics). FT-IR spectra (ExcaliburTM series, Varian Inc.) analysis was used to confirm the characteristic bands of the synthesized nanoparticles. The saturation of magnetization was evaluated using a vibrating sample magnetometer (VSM; MODEL-7300, Lakeshore). The crystallinity of the MNPs and MSNPs was investigated by x-ray diffraction (ESCALAB 220i-XL, VG Scientific).

2.5. Cytotoxicity test of FMSNPs

MDA-MB-231 cells were obtained from ATCC, Manassas, VA. The cytotoxicity of FMSNPs was evaluated by measuring the inhibition of cell growth using the MTT assay. Briefly, cells were plated at a density of 4×10^3 cells ml^{-1} in 96-well plates and treated with FMSNPs at concentrations from 10^{-4}–10^0 mg ml^{-1} for 72 h. Cell viabilities were obtained by calculating the ratio of the number of viable cells in the treated culture compared with non-treated control cells. Every experiment was conducted in triplicate.

2.6. Cell affinity test of FMSNPs

For evaluation of the cellular affinity of FMSNPs, MDA-MB-231 cells were maintained in 5% CO_2 humidified atmosphere at 37 °C in a medium containing 10% (v/v) fetal bovine serum, 100 U ml^{-1} penicillin and 0.1 mg ml^{-1} streptomycin. 1×10^6 cells incubated with FMSNPs in previously described media at 37 °C for 4 h and washed twice with PBS were then collected by trypsinization. The resultant was washed three times with 0.2% FBS and 0.02% NaN_3 in PBS. These samples were resuspended in 400 μl, 4% paraformaldehyde and scanning of the cell-associated fluorescence was performed using a FACScalibur machine (Beckton-Dickinson, Mansfield, MA) at the wavelength $\lambda = 488$ nm.

2.7. MR imaging procedure

MR imaging experiments were performed with a 1.5 T clinical MRI instrument with a micro-47 surface coil (Intera, Philips Medical Systems). R2 relaxivities of MSNPs were measured at room temperature by the Carr–Purcell–Meiboom–Gill (CPMG) sequence: TR = 10 s, 32 echoes with 12 ms even echo space, number of acquisition = 1, point resolution of 156 μm × 156 μm, section thickness of 0.6 mm. R2 is defined as $1/T2$ with units of s^{-1}.

3. Results and discussion

Monodisperse magnetic nanoparticles (MNPs) were synthesized by the thermal decomposition method. The MNPs were capped with dodecanoic acid and the size was approximately 12 nm (figure 2(a)). To increase the magnetic content of magnetic silica nanoparticles (MSNPs), magnetic kernels (MKs) were prepared using MNPs by the nanoemulsion method. The hydrophobic MNPs were assembled using amphiphilic polyvinylalcohol as a surfactant. The size of the spherical MKs measured by laser scattering was 32.7 ± 5.3 nm (figure 3). The MKs were then covered with a silica outer shell by hydrolysis and condensation of TEOS (figure 2(b)). MKs played the role of seeds to induce the formation of spherical MSNPs. The size of the MSNPs was 57.5 ± 7.3 nm and the zeta potential of the MSNPs was -37.3 ± 5.1 mV. The surface charge was shifted from near zero to a negative value due to successful formation of a silica layer coating the non-ionic PVA.

Figure 4(a) shows the FT-IR spectrum of MSNPs. The Fe–O peak of magnetite appeared at 575 cm^{-1} and the spectrum of the Si–O band caused by silica nanoparticles was presented at 1020 cm^{-1} [17]. The crystallinity of MNPs and the presence of silica in MSNPs could be evaluated using XRD patterns (figure 4(b)). Although the MKs were located in the core part of MSNPs, the crystallinity was still maintained.

For assessment of the magnetic properties and sensitivity of the formulated MSNPs, magnetic hysteresis loops were

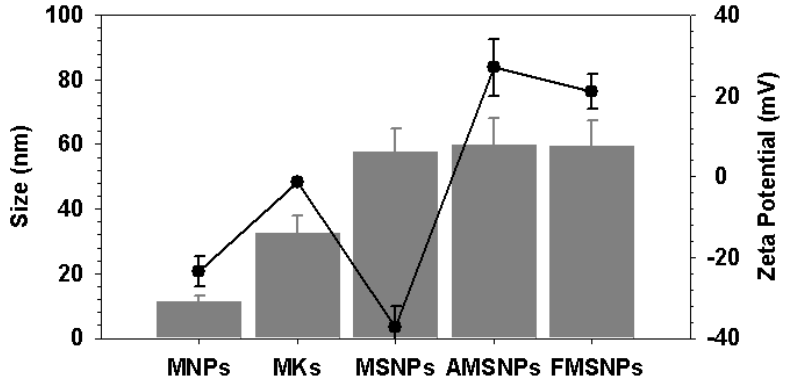

Figure 3. Size and zeta potentials of MNPs, MKs, MSNPs, AMSNPs and FMSNPs. Analysis was conducted in triplicate and the result is expressed as mean value ± standard deviation.

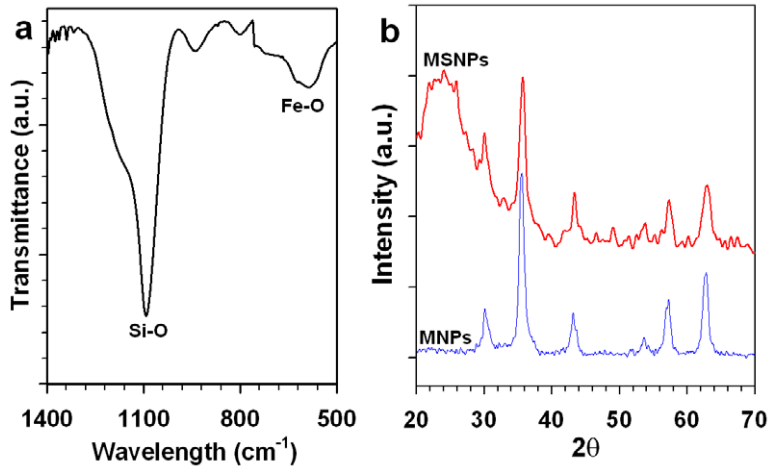

Figure 4. (a) FT-IR spectrum of MSNPs. (b) XRD patterns of MNPs and MSNPs.

recorded using a vibrating sample magnetometer, and MR signal intensities were obtained. The prepared magnetic nanoparticles (MNPs and MSNPs) exhibited a superparamagnetic behavior without magnetic hysteresis (figure 5(a)) at 300 K. The saturation of magnetization (M_s) of MNPs and MSNPs was 73.6 and 47.5 emu g^{-1} at 1.5 T, respectively. The M_s of MSNPs was lower than that of MNPs due to the presence of the silica outer shell. In figure 5(b), the different colors in the MR image represent different concentrations of MSNPs. As the concentration of MSNP increased the T2-weighted MR images exhibited darker color. The relaxivity of MSNPs was 336.1 mM^{-1} s^{-1} (figure 5(c)). These results demonstrated that the MKs enhanced the relaxivity of MSNPs in comparison with previous works [18–20].

To prepare the fluorescent MSNPs, the surfaces of the MSNPs were modified with APTMS. The amine group containing APTMS was conjugated with MSNPs at 90 °C for 24 h. Due to the presence of the amine group, the amine terminated MSNPs (AMSNPs) presented a positive charge. The zeta potential of AMSNPs was 27 ± 7.1 mV (figure 3). However, the size of AMSNPs remained unchanged compared with MSNPs. In order to prepare FMSNPs, the isothiocyanate group of FITC was conjugated with the amine group of the AMSNPs. Although the surface charge of FMSNPs slightly decreased with 21 ± 4.3 mV, the positive charge was still maintained. FMSNPs were well dispersed in the aqueous medium and a fluorescent green color was emitted due to the presence of conjugated FITC on the surface of the MSNPs (figure 6(a)). To investigate the magnetic sensitivity of FMSNPs, a Nd–Fe–B magnet (0.35 T) was applied and we observed that the FMSNPs were aligned along the magnetic field (figure 6(b)).

To apply FMSNPs as magnetic and optical imaging probes, the cytotoxicity of FMSNPs against MDA-MB-231 cells was investigated using an MTT assay. At high concentration of FMSNPs, the cell viability was not decreased (figure 7(a)). For evaluation of cellular binding affinities of FMSNPs against MDA-MB-231 cells, on the other hand, we performed a fluorescence activated cell sorting (FACS) analysis. As seen in figures 7(b) and (c), MDA-MB-231 cells treated with FMSNPs exhibited 16 times higher fluorescence intensity in comparison to non-treated MDA-MB-231 cells. The cationic FMSNPs were attached on the

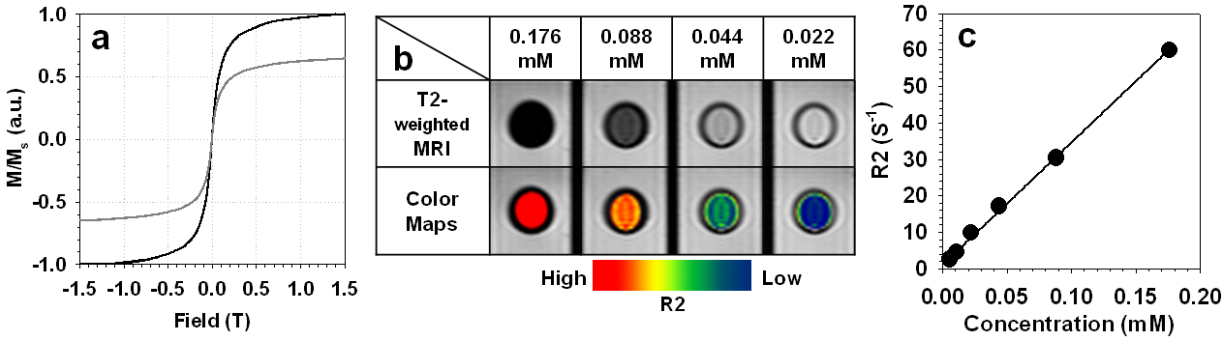

Figure 5. (a) Magnetic hysteresis loops of MSNPs using a vibrating sample magnetometer. (b) T2-weighted MR images and their color maps of MSNPs in aqueous solution. (c) Graph of R2 versus the iron concentration in MSNPs.

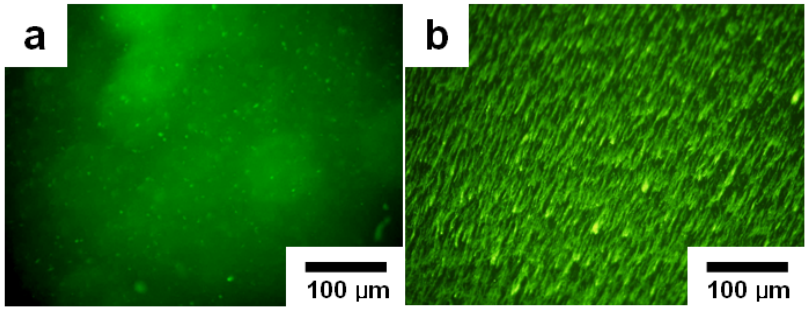

Figure 6. Microscopic images of FMSNPs; (a) without external magnetic field and (b) with external magnetic field.

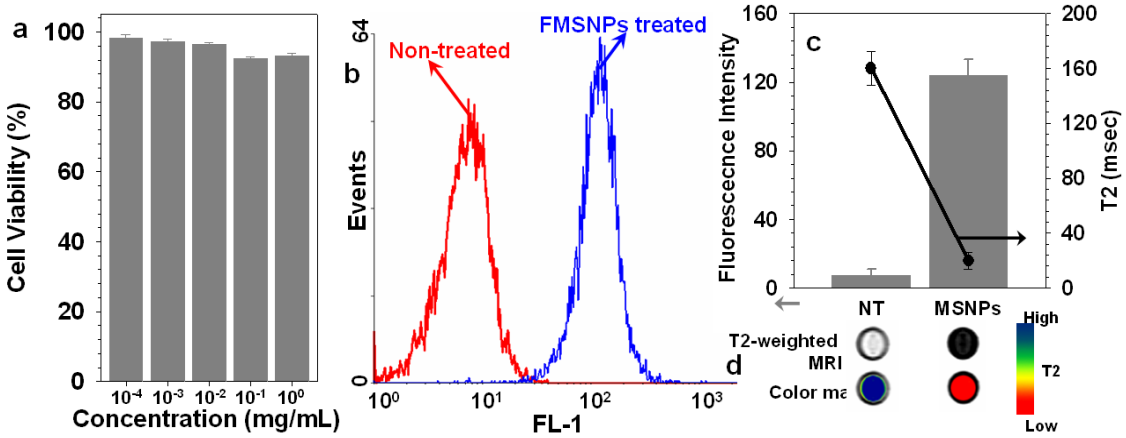

Figure 7. (a) Cell viability graph against concentration of FMSNPs. (b) FACS analysis of MDA-MB-231 treated with FMSNPs. (c) Relative fluorescence intensity and T2 graph of MDA-MB-231 cells treated with FMSNPs and non-treated MDA-MB-231 cells. (d) T2-weighted MR images of MDA-MB-231 cells treated with FMSNPs and non-treated MDA-MB-231 cells.

anionic cell membrane by ionic interaction [21–23]. Moreover, similar results could be verified by MR imaging. The T2-weighted MR image of MDA-MB-231 cells incubated with FMSNPs exhibited a black color compared with the non-treated cells and the calculated T2 values were 20.7 and 160.3 ms, respectively (figure 7(c)). The corresponding color maps for MR images of MDA-MB-231 cells are presented in figure 7(d) and the results demonstrated analogous results with those of the FACS analysis. In figure 7(d), MDA-MB-231 cells incubated with FMSNPs exhibited red color and non-treated MDA-MB-231 cells demonstrated blue color. The red color means the low T2 value and blue color represents the high T2 value.

To assess the magnetic sensitivity of FMSNPs as biomedical imaging probes, MDA-MB-231 cells treated with FMSNPs were injected into a borosilicate micro-channel (square inner diameter 500 μm). Then, magnetic mobilities induced by a Nd–B–Fe magnet (0.35 T) against MDA-MB-231 cells incubated with FMSNPs were investigated using fluorescence microscopic images. In figure 8(a), we could observe the green and blue colors of MDA-MB-231 cells. The green color represented the attached FMSNPs on the

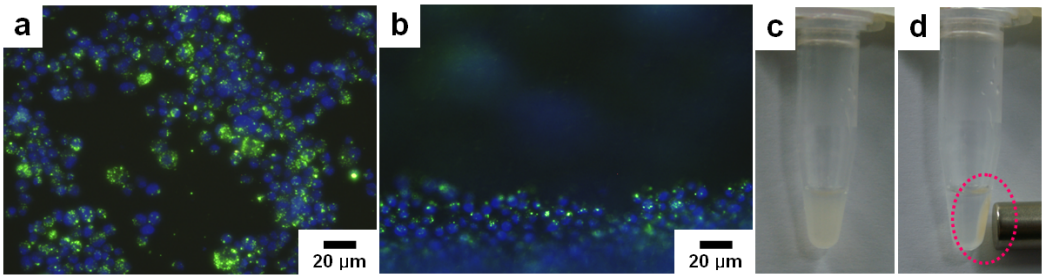

Figure 8. The fluorescence microscopic images of MDA-MB-231 cells treated with FMSNPs: (a) dispersed in the medium and (b) with a magnetic field applied with a Nd–B–Fe magnet; (c) dispersed in a microtube and (d) with the magnetic field applied.

surface of cell and blue color meant the nuclear site of cell stained by 4′, 6-diamidino-2-phenylindole. When the external magnetic field was applied, MDA-MB-231 cells treated with FMSNPs moved towards the magnet (figure 8(b)). These results indicated that FMSNPs exhibited acceptable cellular binding efficiency. Furthermore, without a magnetic field, MDA-MB-231 cells treated with FMSNPs were well dispersed in the PBS of the polymerase chain reaction tube, however the cells collected at the side wall soon after the magnet was placed (figures 8(c) and (d)). Thus, FMSNPs had a sufficient sensitivity to external magnetic fields for many biomedical applications such as MR imaging and cell separations.

4. Conclusions

In summary, we have synthesized novel fluorescent magnetic silica nanoparticles (FMSNPs) for biomedical application. To prepare magnetic silica nanoparticles (MSNPs) containing large magnetic components, the magnetic assembles as kernels were encapsulated with silica. Thus, the prepared MSNPs exhibited superparamagnetic behavior and the saturation of magnetization and MR signal intensity of MSNPs were significantly increased. After conjugation of a fluorescent dye on the surface of amine terminated MSNP, the FMSNPs demonstrated potential as multimodal imaging probes. The cellular binding efficiency of FMSNPs was improved because of the interaction between positively charged FMSNPs and the cell membrane. Consequently, target cells treated with FMSNPs could be detected by MRI and fluorescence microscopy. Furthermore, the target cells treated with FMSNPs were sensitively reacted under an external magnetic field. These results demonstrated the highly efficient ability for biomedical applications. Therefore, with respect to economical efficiency, simplicity and reproducibility on a large scale, this study could be used as a novel strategy for many biomedical applications using magnetic nanoparticles.

Acknowledgments

This work was supported by the Korea Science and Engineering Foundation (KOSEF) (R15-2004-024-00000-0, M10755020001-07N5502-00110 and R01-2006-000-10023-0) and a grant from the National R&D Program for Cancer Control, Korea Ministry of Health and Welfare (0620190-1).

References

[1] Yang J, Lee C H, Park J, Seo S, Lim E K, Song Y J, Suh J S, Yoon H G, Huh Y M and Haam S 2007 *J. Mater. Chem.* **17** 2695
[2] Song H T, Choi J S, Huh Y M, Kim S, Jun Y W, Suh J S and Cheon J 2005 *J. Am. Chem. Soc.* **127** 9992
[3] Schneider T, Moore L R, Jing Y, Haam S, Williams P S, Fleischman A J, Roy S, Chalmers J J and Zborowski M 2006 *J. Biochem. Biophys. Methods* **68** 1
[4] Yang H H, Zhang SQ, Chen X L, Zhuang Z X, Xu J G and Wang X R 2004 *Anal. Chem.* **76** 1316
[5] Jun Y W *et al* 2005 *J. Am. Chem. Soc.* **127** 5732
[6] Huh Y M *et al* 2005 *J. Am. Chem. Soc.* **127** 12387
[7] Lee J *et al* 2006 *Nat. Med.* **13** 95
[8] Suzuki M, Shinkai M, Honda H and Kobayashi T 2003 *Melanoma Res.* **13** 129
[9] Philipse A P, Bruggen M and Pathmamanoharan C 1994 *Langmuir* **10** 92
[10] Deng Y H, Wang C C, Hu J H, Yang W L and Fu S K 2005 *Colloids surf.* A **262** 87
[11] Sun S, Zeng H, Robinson D B, Raoux S, Rice P M, Wang S X and Li G 2004 *J. Am. Chem. Soc.* **126** 273
[12] Yoon T J, Kim J S, Kim B G, Yu K N, Cho M H and Lee J K 2005 *Angew. Chem. Int. Edn* **44** 1068
[13] Lee J H, Jun Y W, Yeon S I, Shin J S and Cheon J 2006 *Angew. Chem. Int. Edn* **45** 8160
[14] Stöber W and Fink A 1968 *J. Colloid Interface Sci.* **26** 62
[15] Pham T, Jackson J B, Halas N J and Lee T R 2002 *Langmuir* **18** 4915
[16] Zhang Y, Kohler N and Zhang M 2002 *Biomaterials* **23** 1553
[17] Xu G Q, Zheng Z X, Tang W M and Wu Y C 2007 *J. Lumin.* **126** 43
[18] Kim J *et al* 2006 *J. Am. Chem. Soc.* **128** 688
[19] Kim J *et al* 2006 *Angew. Chem.* **118** 7918
[20] Perez J M, Josephson L, O'Loughlin T, Högemann D and Weissleder R 2002 *Nat. Biotechnol.* **20** 816
[21] Fewell J G, Matar M, Slobodkin G, Han S O, Rice J, Hovanes B, Lewis D H and Anwer K 2005 *J. Control. Release* **109** 288
[22] Son K K, Tkach D and Patel D H 2000 *Biochim. Biophys. Acta* **1468** 11
[23] Zhdanov R I, Podobed O V and Vlassov V V 2002 *Bioelectrochemistry* **58** 53